The iminosugar AMP-DNM improves satiety and activates brown adipose tissue through GLP1

Moro Chao, D.H.; Wang, Y.; Foppen, E.; Ottenhoff, R.; Roomen, C. van; Parlevliet, E.T.; ... ; Yi, C.X.

The Iminosugar AMP-DNM Improves Satiety and Activates Brown Adipose Tissue Through GLP1

Daniela Herrera Moro Chao,[1,2] Yanan Wang,[3] Ewout Foppen,[2] Roelof Ottenhoff,[1] Cindy van Roomen,[1] Edwin T. Parlevliet,[3] Marco van Eijk,[4] Marri Verhoek,[4] Rolf Boot,[4] Andre R. Marques,[4] Saskia Scheij,[1] Mina Mirzaian,[4] Sander Kooijman,[3] Kirstin Jansen,[2] Dawei Wang,[5,6] Clarita Mergen,[7] Randy J. Seeley,[8] Matthias H. Tschöp,[7] Herman Overkleeft,[9] Patrick C.N. Rensen,[3] Andries Kalsbeek,[2,5] Johannes M.F.G. Aerts,[4] and Chun-Xia Yi[2]

Diabetes 2019;68:2223–2234 | https://doi.org/10.2337/db19-0049

Obesity is taking on worldwide epidemic proportions, yet effective pharmacological agents with long-term efficacy remain unavailable. Previously, we designed the iminosugar N-adamantine-methyloxypentyl-deoxynojirimycin (AMP-DNM), which potently improves glucose homeostasis by lowering excessive glycosphingolipids. Here we show that AMP-DNM promotes satiety and activates brown adipose tissue (BAT) in obese rodents. Moreover, we demonstrate that the mechanism mediating these favorable actions depends on oral, but not central, administration of AMP-DNM, which ultimately stimulates systemic glucagon-like peptide 1 (GLP1) secretion. We evidence an essential role of brain GLP1 receptors (GLP1r), as AMP-DNM fails to promote satiety and activate BAT in mice lacking the brain GLP1r as well as in mice treated intracerebroventricularly with GLP1r antagonist exendin-9. In conclusion, AMP-DNM markedly ameliorates metabolic abnormalities in obese rodents by restoring satiety and activating BAT through central GLP1r, while improving glucose homeostasis by mechanisms independent of central GLP1r.

Obesity and associated complications are among the most significant world's public health problems. Unfortunately, to date, approved antiobesity pharmacological treatments are still extremely limited. Iminosugars are sugar analogs in which nitrogen replaces the oxygen in the ring structure. Numerous natural and synthetic iminosugars have been shown to inhibit enzymes involved in the metabolism of glycosphingolipids (GSLs) (1). Built on the evidence demonstrating that excessive GSLs are implicated in the onset of metabolic comorbidities of obesity (1,2), our group designed the amphiphilic iminosugar N-adamantine-methyloxypentyl-deoxynojirimycin (AMP-DNM), which efficiently improves glucose homeostasis by enhancing insulin sensitivity (3,4), reduces inflammation of adipose tissue, and corrects hepatosteatosis (1,5,6) in obese rodents by inhibiting the biosynthesis of glucosylceramide and consequently reducing GSLs. In the current study, we thoroughly investigated the physiological and molecular mechanism by which AMP-DNM exerts its beneficial metabolic effects. We here report that AMP-DMN is an orally active satietogenic compound whose action is relayed by

[1]Department of Medical Biochemistry, Amsterdam UMC, University of Amsterdam, Amsterdam, the Netherlands
[2]Laboratory of Endocrinology, Department of Endocrinology and Metabolism, Amsterdam Gastroenterology & Metabolism, Amsterdam UMC, University of Amsterdam, Amsterdam, the Netherlands
[3]Division of Endocrinology and Einthoven Laboratory for Experimental Vascular Medicine, Department of Medicine, Leiden University Medical Center, Leiden, the Netherlands
[4]Department of Medical Biochemistry, Leiden Institute of Chemistry, Leiden, the Netherlands
[5]Hypothalamic Integration Mechanisms, Netherlands Institute for Neuroscience, Amsterdam, the Netherlands
[6]Institute of Plant Protection, Chinese Academy of Agricultural Science, Beijing, China
[7]Helmholtz Diabetes Center and German Center for Diabetes Research, Helmholtz Zentrum München, Neuherberg, Germany, and Division of Metabolic Diseases, Technische Universität München, Munich, Germany
[8]Department of Surgery, University of Michigan, MI
[9]Department of Bio-organic Synthesis, Leiden Institute of Chemistry, Leiden, the Netherlands

Corresponding author: Johannes M.F.G. Aerts, j.m.f.g.aerts@lic.leidenuniv.nl

Received 6 February 2019 and accepted 21 September 2019

This article contains Supplementary Data online at http://diabetes.diabetesjournals.org/lookup/suppl/doi:10.2337/db19-0049/-/DC1.

D.H.M.C. and Y.W. contributed equally to this work. J.M.F.G.A. and C.-X.Y. contributed equally this work.

systemic release of GLP1. We show that AMP-DMN increases activation of brown adipose tissue (BAT) and decreases food intake by essentially involving central GLP1 signaling pathways. Altogether, our work depicts a comprehensive action of AMP-DMN that promotes beneficial metabolic and insulin-sensitizing action through both GLP1-dependent and -independent pathways.

RESEARCH DESIGN AND METHODS

Animals

All animals used in the study were males and were kept in individual cages at constant temperature (23 ± 2°C), submitted to a 12-h/12-h light/dark cycle. They were exposed to ad libitum food and water before and after the experimental procedures, except when mentioned otherwise. Conditional Nkx2.1-Cre GLP1r flox/flox (GLP1r KD$^{\Delta Nkx2.1}$) mice were generated after crossing of GLP1r$^{lox/lox}$ mice (7) with Nkx2.1-Cre mice (The Jackson Laboratory, Bar Harbor, ME). Nkx2.1-Cre mice were used as wild-type (wt) control.

Iminosugars

AMP-DNM and L-ido-AMP-DNM were synthesized at the Leiden Institute of Chemistry as previously described (4).

Surgical Procedures

Wistar rats (8–10 weeks old, Harlan Laboratories, Horst, the Netherlands) and ZDF rats (8–10 weeks old, Charles River Laboratories, Chatillon-sur-Chalaronne, France) were anesthetized with a mixture of 0.4 mL/kg Dormicum (Roche, Almere, the Netherlands) and 0.8 mL/kg Hypnorm (Janssen, Buckinghamshire, U.K.). For infusions in the central nervous system (CNS), intracerebroventricular (icv) stainless steel guide cannulas were implanted into the lateral ventricle using the following stereotaxic coordinates: AP −0.9, L 2.0, and V −3.4, tooth bar (−2.5 mm). For the peripheral infusions, intragastric (ig) silicon cannulas were implanted into the stomach. Additional groups of Wistar and ZDF rats were implanted with an ig and a right jugular vein catheter during the same surgery for simultaneous ig infusions and intravenous blood sampling (8). Analgesic Buprecare (Recipharm, Lancashire, U.K.) was administered after the animals woke up from the surgery; experiments were performed after a period of 7–10 days postoperative recovery. C57Bl/6J mice were implanted with icv cannulas in the lateral ventricle connected to osmotic minipumps (model 1004, Alzet) as previously described (9). The minipumps were filled with exendin-9 or artificial cerebral spinal fluid (aCSF) and assured continuous delivery of 0.72 mmol/kg/day exendin-9 (10).

Iminosugar Infusions in Rats

After the postsurgical recovery period, rats were transferred to an indirect calorimetry system (TSE Systems, Bad Homburg, Germany). Food intake, locomotor activity, energy expenditure (EE), respiratory exchange ratio (RER), and fatty acid and carbohydrate oxidation rates were assessed as previously described (8,11). After a 4-day acclimation period, the rats were icv (0.03 mg/kg) or ig (100 mg/kg) infused with AMP-DNM (Wistar group, icv $n = 8$, ig $n = 4$; ZDF group, icv $n = 5$, ig $n = 7$), L-ido-AMP-DNM (Wistar, icv $n = 7$, ig $n = 4$; ZDF, icv $n = 4$, ig $n = 5$), or vehicle (Wistar, icv $n = 6$, ig $n = 4$; ZDF, icv $n = 5$, ig $n = 5$) on days 5 and 7; the animals were not disturbed during days 6, 8, and 9 until they were sacrificed by CO_2 euthanasia. An additional pair-fed (PF) ZDF group was administered ig AMP-DNM ($n = 6$) or vehicle ($n = 5$). Tail cuts for blood sampling were performed on day 5 as well as on day 9 for plasma hormone measurement and glucose assessment using a glucometer (Freestyle Freedom-Lite, Abbott, Hoofddorp, the Netherlands).

Iminosugar Infusions in Mice

C57Bl/6J wt lean and *ob/ob* mice (8–10 weeks old) (Envigo, Venray, the Netherlands) were fasted for 3 h and then ig infused with AMP-DNM (100 mg/kg) (wt, $n = 4$; *ob/ob*, $n = 8$) or vehicle (wt, $n = 7$; *ob/ob*, $n = 5$). The mice were sacrificed 90 min later and transcardially perfused with 250 mL 0.9% (w/v) saline solution followed by 4% paraformaldehyde in phosphate buffer (0.1 mol/L, pH 7.2). Brains were processed for immunohistochemistry. Additional groups of mice received oral gavage of AMP-DNM (100 mg/kg) (wt, $n = 7$; *ob/ob*, $n = 6$) or vehicle (wt, $n = 5$; *ob/ob*, $n = 5$) 3 h after food had been removed. Two hours later the mice were sacrificed, and their brains were removed and frozen for analysis. For investigation of the peripheral GLP1 response after AMP-DNM, two groups of C57Bl/6J wt lean mice received an oral gavage of AMP-DNM (100 mg/kg) ($n = 6$) or vehicle ($n = 8$) 6 h after food had been removed. Blood was collected at 20, 40, and 60 min after infusion of AMP-DNM, and active GLP1 in plasma was analyzed by ELISA (K1503OD; Meso Scale Discovery).

Chronic AMP-DNM Administration to Mice

C57Bl/6J wt mice were fed with a high-fat diet (HFD) (cat. no. D12492, Research Diets, New Brunswick, NJ) for 12 weeks and then were placed individually in metabolic cages for 3 days for basal assessment of metabolic parameters. Afterward animals were fed with an HFD ($n = 10$) or an HFD with AMP-DNM ($n = 9$) mixed in the food (HFD+AMP-DNM [100 mg/kg]) for 4 weeks. Body weight and food intake was measured daily. A PF group ($n = 5$) was included, matched to HFD+AMP-DNM. Additional groups of animals were implanted with an icv cannula, via which they received aCSF ($n = 5$) or exendin-9 ($n = 7$). In the second week of treatment, an oral glucose tolerance test (OGTT) was performed. In week 4, animals were fasted for 4 h and were infused with a mixture of glycerol tri[^{3}H]oleate-labeled triglyceride (TG)-rich lipoprotein (TRL)-like particles and 2-[1-^{14}C]deoxy-D-glucose ([^{14}C]DG) for assessment of TG and glucose clearance as previously described (9). Mice were sacrificed by cervical dislocation

followed by immediate body composition (lean and fat mass) measurement with an EchoMRI-100 (EchoMRI, Houston, TX), and afterward organs were collected for further analysis.

GLP1r KD$^{\Delta Nkx2.1}$, GLP1r knockout (GLP1r KO) (Drucker lab) (12), and wt mice were fed with an HFD for 8 weeks and then individually placed in metabolic cages for 4 days for basal metabolic parameter assessment. Afterward, the animals were divided into an HFD-fed group (GLP1r KD$^{\Delta Nkx2.1}$, $n = 5$; GLP1r KO, $n = 6$; and wt, $n = 13$) and HFD+AMP-DNM-fed (100 mg/kg) group (GLP1r KD$^{\Delta Nkx2.1}$, $n = 6$; GLP1r KO, $n = 6$; and wt, $n = 14$) and remained in the metabolic cages for another 5 days. After this period, an OGTT was performed in week 3 after exposure to HFD+AMP-DNM diet. At the end of week 4, animals were fasted for 4 h and animals fed HFD received a vehicle oral gavage, while the animals fed HFD+AMP-DNM received an AMP-DNM oral gavage. Next, mice were sacrificed and their brains and BAT were removed for immunohistochemistry and gene expression analysis.

Statistical Analysis

Results are expressed as the mean ± SEM. Two-way ANOVA, one-way ANOVA, and *t* test analysis were performed using SPSS, version 19, and GraphPad Prism 6. Pairwise comparisons were evaluated with a Tukey and Fisher's least significant difference post hoc test.

Study Approval

All animal protocols were approved by the animal ethics committee of the government of Upper Bavaria (Germany), the Institutional Animal Welfare Committee of the Academic Medical Center and the Royal Netherlands Academy of Arts and Science (University of Amsterdam) and the Leiden University Medical Center.

Data and Resource Availability

All data generated or analyzed during this study are included here (and in Supplementary Data). The iminosugars generated during the current study are available from the corresponding author upon reasonable request.

RESULTS

Peripheral Administration of AMP-DNM Reduces Body Weight Gain, Decreases Food Intake, and Increases Fat Oxidation in Obese Rats

First, we studied the effects of peripheral ig administration of AMP-DNM (Fig. 1*A*) in lean rats. While food intake during 5 days was not changed (Fig. 1*B*), the RER was decreased (Fig. 1*C*), fat oxidation was increased (Fig. 1*D*), and body weight gain was reduced (Fig. 1*E*). Energy expenditure (data not shown), locomotor activity (data not shown), and plasma glucose (Fig. 1*F*) were not changed by ig treatment. In obese diabetic ZDF rats, AMP-DNM administered ig decreased daily food intake (Fig. 1*G*), decreased RER (Fig. 1*H*), increased fat oxidation rate (Fig. 1*I*), and reduced body weight gain (Fig. 1*J*). Hyperglycemia was lowered in obese ZDF rats receiving AMP-DNM (Fig. 1*K*). Of note, in another experiment reduced food intake was also observed in rats exposed long-term to AMP-DNM via their food (Supplementary Fig. 1*A*).

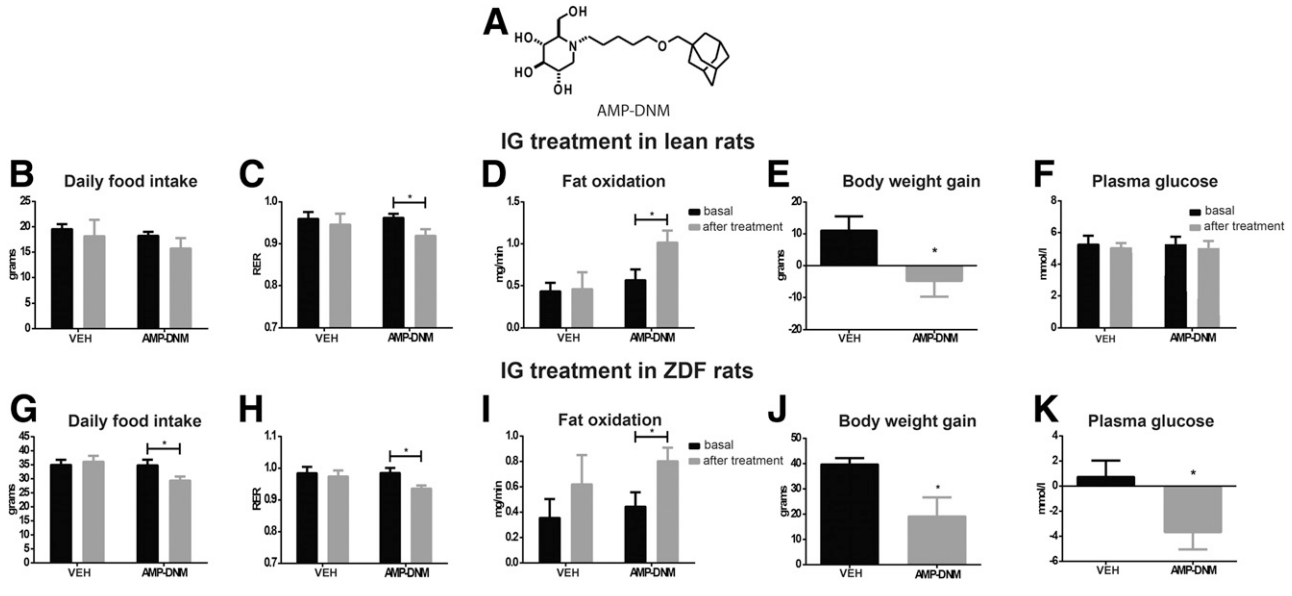

Figure 1—ig AMP-DNM administration increases fat oxidation in lean rats and obese ZDF rats and decreases food intake and plasma glucose levels in obese ZDF rats. *A*: Chemical structure of AMP-DNM. AMP-DNM or vehicle was administered by gavage (ig). *B*: Daily food intake of lean rats. *C*: RER of lean rats. *D*: Fat oxidation in lean rats. *E*: Body weight gain of lean rats. *F*: Plasma glucose levels of lean rats. *G*: Daily food intake of obese ZDF rats. *H*: RER of ZDF rats. *I*: Fat oxidation in ZDF rats. *J*: Body weight gain in ZDF rats. *K*: Plasma glucose levels after AMP-DNM ig in ZDF rats. VEH, vehicle administration. *$P < 0.05$.

To establish whether the metabolic improvements in the ad libitum ig AMP-DNM–treated obese ZDF rats were caused by their decreased food intake, we had an additional PF group. RER was lower in PF animals (Supplementary Fig. 1*B*), and body weight gain tended to be less (Supplementary Fig. 1*C*). However, PF animals did not show the changes in fat oxidation and plasma glucose (data not shown) imposed by AMP-DNM. Clearly, reduced food intake does not explain all metabolic improvements induced by AMP-DNM in the obese rats. To determine whether the observed improvements induced by AMP-DNM are due to a direct action in the brain, central icv infusions of AMP-DNM were performed in lean and obese rats. None of the investigated parameters were significantly changed (Supplementary Fig. 1*D–M*). Thus, AMP-DNM acts peripherally to increase fatty acid substrate utilization and decrease body weight gain in lean as well as obese rats.

AMP-DNM Stimulates Hypothalamic and Brainstem Anorexigenic Peptide Expression

We next examined whether ig administration of AMP-DNM causes activation of hypothalamic and brainstem nuclei by analyzing C-Fos immunoreactivity (IR) in brains of lean and *ob/ob* mice after ig administration of AMP-DNM. AMP-DNM increased C-Fos IR in the hypothalamic arcuate nucleus (ARC) (Fig. 2*A* and *B*) and in the dorsomedial hypothalamic nucleus (DMH) (Fig. 2*C* and *D*), as well as in the nucleus of the tractus solitaris (NTS) (Fig. 2*E* and *F*) of both lean and *ob/ob* mice. The same was observed for the area postrema (AP) (mice: vehicle lean 15.18 ± 2.10 and obese 14.3 ± 3.70; AMP-DNM, lean 63 ± 19.61 and obese 154.57 ± 8.27) (lean, $P = 0.0241$; obese, $P < 0.0001$). *ob/ob* mice presented higher activation of C-Fos in the ARC, DMH, and AP compared with lean mice (Fig. 2*A* and *C*); such a higher increase was not observed in the NTS (Fig. 2*E*). Double immunofluorescence revealed that anorexigenic neuronal populations such as pro-opiomelanocortin (POMC) neurons in the ARC (Supplementary Fig. 2*A* and *B*) and GLP1 neurons in the NTS (Supplementary Fig. 2*C* and *D*) were activated after AMP-DNM ig administration. Next, we studied microdissected ARC, paraventricular nucleus (PVN), DMH, lateral hypothalamus (LH), and NTS of lean and *ob/ob* mice ig infused with AMP-DNM (Supplementary Fig. 3*A* and *B*). Neuropeptide Y (NPY), Agouti-related peptide, and POMC expression in the ARC of lean mice did not differ after AMP-DNM

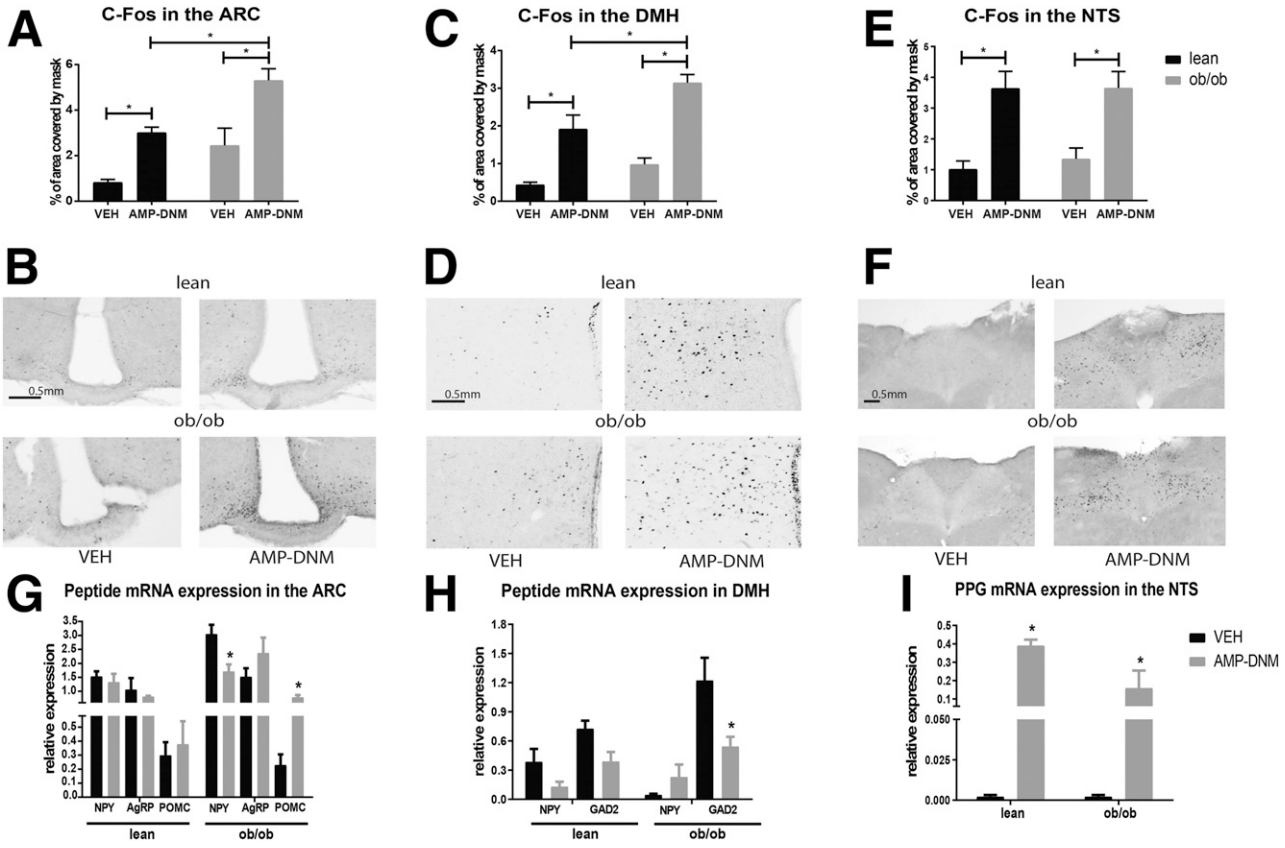

Figure 2—ig AMP-DNM administration activates the hypothalamus and brainstem neurons and increases anorexigenic neuropeptide expression in the ARC and NTS. *A*: Percentage of ARC area covered by C-Fos. *B*: C-Fos IR representative images in the ARC. *C*: Percentage of DMH area covered by C-Fos mask. *D*: C-Fos IR representative images in the DMH. *E*: Percentage of NTS area covered by C-Fos mask. *F*: C-Fos IR representative images in the NTS. *G*: Neuropeptide mRNA expression in the ARC. *H*: Neuropeptide mRNA expression in the DMH. *I*: PPG mRNA expression in the NTS. VEH, vehicle administration. Scale bar: 0.5 mm. *$P < 0.05$.

administration; however, the ARC of *ob/ob* mice showed significantly reduced levels of NPY and increased levels of POMC expression (Fig. 2*G*). In the DMH of AMP-DNM–treated *ob/ob* mice, but not lean mice, a significant decrease of GAD2 expression was observed (Fig. 2*H*). Expression of NPY did not differ in the DMH of AMP-DNM–treated *ob/ob* and lean mice. Likewise, in the lateral hypothalamus of lean and *ob/ob* mice, the expression of NPY, GAD2, orexin, and Melanin-concentrating hormone was not changed by AMP-DNM treatment (Supplementary Fig. 3*C*). In the PVN of lean and *ob/ob* mice, the expression of thyroid-releasing hormone and oxytocin was unaffected by AMP-DNM treatment. A decrease in corticotropin-releasing hormone expression was found after AMP-DNM oral administration to *ob/ob* mice (mRNA relative expression after vehicle 0.783 ± 0.2647 or after AMP-DNM 0.211 ± 0.041) (Supplementary Fig. 3*D*). Finally, expression of preproglucagon (PPG) in the NTS was found to be increased after AMP-DNM administration in both lean and *ob/ob* mice (Fig. 2*I*). In conclusion, AMP-DNM significantly influences hypothalamic-brainstem anorexigenic circuits, including the ARC, DMH, and NTS.

AMP-DNM Reduces Body Weight Gain and Improves Glucose Homeostasis in Mice With Diet-Induced Obesity

Next, we investigated the potential ameliorative effects of AMP-DNM in mice with HFD-induced obesity (DIO mice), including an additional PF group. DIO mice fed with AMP-DNM–containing diet presented reduced food intake (Fig. 3*A*). The reduced food intake induced by AMP-DNM was accompanied by a decrease in body weight gain that exceeded that in the PF group (Fig. 3*B*). Analysis of body composition showed a decrease in fat mass gain and

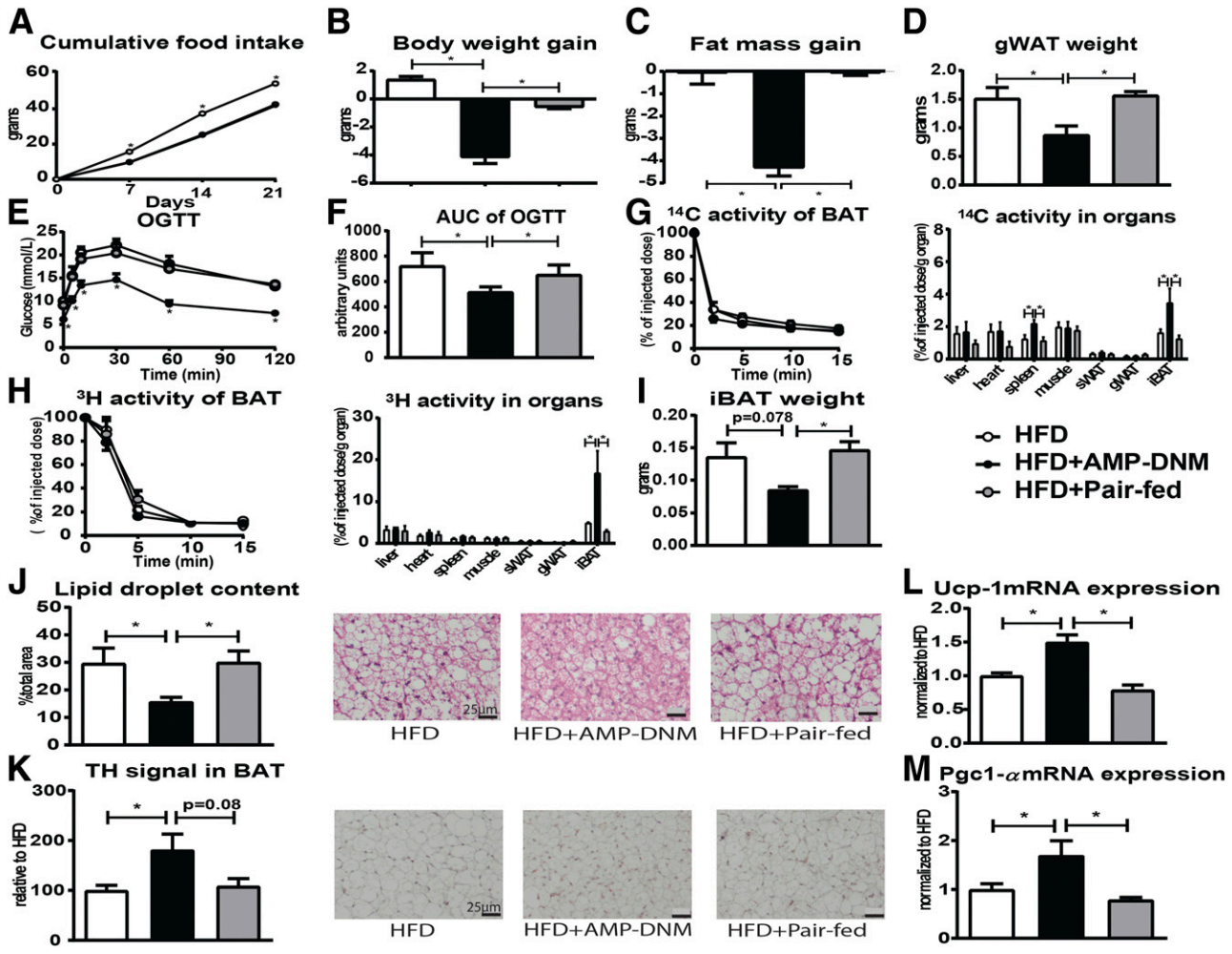

Figure 3—Chronic AMP-DNM administration ameliorates obesity, improves glycemia, and stimulates BAT activity in obese mice. *A*: Cumulative food intake. *B–D*: Difference in body weight gain, fat mass gain, and gWAT pad weight. *E* and *F*: Plasma glucose levels and AUC after an OGTT. *G*: Plasma ^{14}C activity decay and tissue ^{14}C activity uptake in mice intravenously infused with [^{14}C]DG. *H*: Plasma ^{3}H activity decay and tissue ^{3}H activity uptake in mice fed HFD or HFD+AMP-DNM and intravenously infused with glycerol tri[^{3}H]oleate–labeled particles. *I*: iBAT pad weight. *J*: Lipid droplet content quantification and representative images of hematoxylin-eosin staining of iBAT. *K*: TH signal quantification and representative images of TH staining of iBAT. *L*: *Ucp-1* mRNA expression in iBAT. *M*: *Pgc1-α* mRNA expression in iBAT. Scale bar: 25 μm. *$P < 0.05$.

a decreased gonadal white adipose tissue (gWAT) weight in the AMP-DNM group but not in the PF group (Fig. 3*C* and *D*). These data suggest that AMP-DNM decreases white adipose tissue mass and body weight via mechanisms different from those of decreased food intake. DIO mice fed HFD+AMP-DNM showed decreased plasma glucose levels after fasting compared with the DIO mice fed HFD ($t = 0$ [in Fig. 3*E*]). OGTT revealed that the AMP-DNM–fed group presented an improved glucose tolerance that was independent of decreased food intake, as was revealed by comparison with PF mice (Fig. 3*E* and *F*). Altogether, these results indicate that AMP-DNM reduces body weight gain and improves glucose homeostasis in obese mice.

AMP-DNM Stimulates BAT Activity

BAT activation is known to improve glucose metabolism and decrease body weight in obese animals (13–15). To investigate whether AMP-DNM modulates BAT activity, [^{14}C]DG and glycerol TRL-like emulsion particles were infused in DIO mice fed with or without addition of AMP-DNM. The uptake of glucose and TG-derived fatty acids in different organs was monitored. Chronic AMP-DNM administration increased the uptake of [^{14}C]DG (Fig. 3*G*) and [^{3}H]oleate (Fig. 3*H*) in interscapular BAT (iBAT). Such increases were not observed in the PF group (Fig. 3*G* and *H*). The increased glucose and TG-derived fatty acid uptake in the BAT of AMP-DNM–fed mice was accompanied by a trend of decreased iBAT weight (Fig. 3*I*) and significantly decreased lipid droplet content (Fig. 3*J*). These findings suggest that chronic administration of AMP-DNM stimulates glucose and fatty acid uptake in iBAT by stimulating combustion of intracellular lipid stores. Increased iBAT activity in DIO mice fed with AMP-DNM was also suggested by an increase of the tyrosine hydroxylase (TH) signal (Fig. 3*K*) and increased expression of thermogenic genes *Ucp-1* and *Pgc-1α* (Fig. 3*L* and *M*).

AMP-DNM Satietogenic Action Is Accompanied by Increased Active GLP1 in Plasma

Based on the finding that ig, but not icv, AMP-DNM influences metabolism, we hypothesized that it may influence gastrointestinal endocrine factors. Indeed, a significantly increased plasma concentration of active GLP1 was observed in lean rats at 20 min, 40 min, and 60 min after infusion of AMP-DNM (Fig. 4*A*). Likewise, ig AMP-DNM administration in obese ZDF rats led to increased plasma concentrations of active GLP1 over time (Fig. 4*B*). The higher plasma GLP1 was accompanied with reduced refeeding after fasting in both lean (Fig. 4*C*) and obese rats (Fig. 4*D*). Similar to the GLP1 induction by AMP-DNM in rats, ig AMP-DNM acutely and transiently increased plasma concentration of GLP1 in mice at 20 min (Supplementary Fig. 4*A*) as well as the area under the curve (AUC) within 60 min (Supplementary Fig. 4*B*). Thus, AMP-DNM stimulates the secretion of active GLP1 in lean and obese rodents, accompanied by decreased food intake.

AMP-DNM Stimulates GLP1 Secretion by Cultured Enteroendocrine Cells Through Stimulation of Intestinal Bitter Receptors

Postprandial nutrients can trigger GLP1 secretion from enteroendocrine cells by taste receptor stimulation

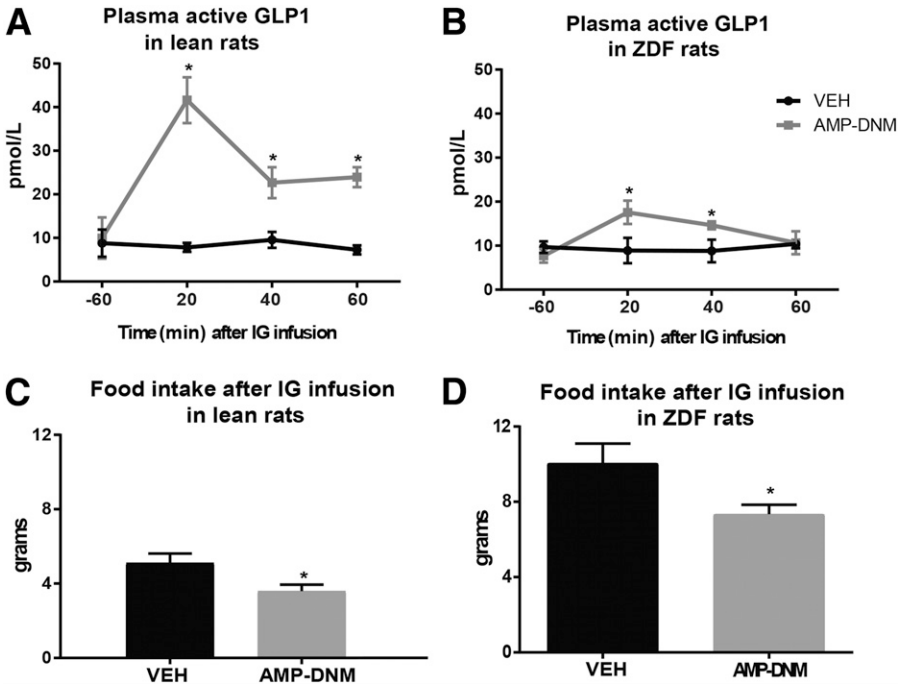

Figure 4—AMP-DNM stimulates intestinal GLP1 secretion. *A*: Plasma GLP1 after AMP-DNM ig in lean rats. *B*: Plasma GLP1 after AMP-DNM ig in obese ZDF rats. Food intake after fasting and AMP-DNM ig in lean (*C*) or ZDF (*D*) rats. VEH, vehicle administration. *$P < 0.05$.

(16,17). The human bitter receptor T2R16 (hT2R16) selectively recognizes β-glucopyranosides (like salicin or gentiobiose) (18,19). We previously showed that the hT2R16 ortholog mouse receptors T2R116 or T2R118 are expressed in the hypothalamus and in the NTS of the brainstem of mice and that their expression is affected by pathological metabolic conditions, like obesity and diabetes (20). We investigated whether AMP-DNM, as hydrophobic β-glycoside, acts on the hT2R16 to stimulate GLP1 secretion from enteroendocrine cells. For comparison, we used the structural analog L-ido-AMP-DNM (Supplementary Fig. 4*C*); L-ido-AMP-DNM inhibits GSL synthesis on a par with AMP-DNM (4) but does not decrease food intake (Supplementary Fig. 5). Likewise, salicin, a bitter glycoside, was examined. For the testing, we overexpressed hT2R16 or GFP in mouse intestinal STC1 cells and measured intracellular Ca^{2+} release and secretion of GLP1 after the exposure of cells to AMP-DNM, L-ido-AMP-DNM, or salicin. As a positive control, we used stimulation with glutamate, a nonbitter stimulus, causing the expected intracellular Ca^{2+} release in GFP- and hT2R16-overexpressing cells (Supplementary Fig. 4*D*). Intracellular Ca^{2+} release in hT2R16 cells was higher after incubation with salicin compared with control cells (Supplementary Fig. 4*E* and *H*). Exposure to AMP-DNM also dose-dependently provoked increased intracellular Ca^{2+} responses in the hT2R16 compared with control cells (Supplementary Fig. 4*F* and *I*). The intracellular Ca^{2+} response coincided with a significant increase of GLP1 in medium of the hT2R16 cells (Supplementary Fig. 4*K*). In contrast, only the highest concentration of 100 μmol/L L-ido-AMP-DNM increased a Ca^{2+} response in hT2R16 cells (Supplementary Fig. 4*G* and *J*), without causing a significant increase of GLP1 in the medium (Supplementary Fig. 4*L*). We next overexpressed the hT2R16 mouse ortholog receptor T2R118 in STC1 cells. Similarly, AMP-DNM increased GLP1 secretion in medium of T2R118-overexpressing cells (Supplementary Fig. 4*M*). Of note, L-ido-AMP-DNM ig or icv treatment did not show any significant changes in the metabolic parameters measured in lean rats or obese ZDF rats (Supplementary Fig. 5), except for a decrease in plasma glucose levels in the obese ZDF rats after ig administration (Supplementary Fig. 5*K*).

The Anorectic Action of AMP-DNM Requires the Integrity of Brain GLP Signaling

To study further the involvement of GLP1 in the metabolic effects of AMP-DNM, we determined the responses to AMP-DNM in wt and GLP1r KO mice on HFD. AMP-DNM induced a decrease in daily food and water intake in DIO wt mice but not in GLP1rKO animals (Fig. 5*A* and *B*). RER was decreased in both wt and GLP1rKO mice fed with AMP-DNM (Fig. 5*C*). Apparently, GLP1r mediates the satiating effect of AMP-DNM but not the decrease in RER. Body weight loss in wt and GLP1rKO mice were similar after 3 weeks' AMP-DNM diet (wt −2.5 ± 1.9 g and GLP1rKO −4.6 ± 1.9 g). GLP1r in the hypothalamus is involved in the beneficial effects of GLP1 on insulin sensitivity, delayed gastric emptying, and improved satiety (21). To test the potential role of central GLP1r, GLP1r $KD^{\Delta Nkx2.1}$ mice and wt animals were studied in their response to AMP-DNM. GLP1r $KD^{\Delta Nkx2.1}$ mice express Cre recombinase throughout most hypothalamic neurons expressing the Nkx2.1 promoter (22). Analysis of Cre expression in GLP1r $KD^{\Delta Nkx2.1}$ mice showed abundant Cre mRNA expression in the hypothalamus (Fig. 5*M*). DIO wt mice showed decreased daily food and water intake after AMP-DNM administration by the diet. However, GLP1r $KD^{\Delta Nkx2.1}$ mice did not reduce their food or water intake after AMP-DNM treatment (Fig. 5*D* and *E*). This finding suggests that GLP1r in the brain crucially mediates the satiety-promoting effect of AMP-DNM. AMP-DNM treatment decreased RER (wt, $P = 0.001$, and GLP1r $KD^{\Delta Nkx2.1}$, $P = 0.004$) (Fig. 5*F*) and improved glucose homeostasis (wt, $P = 0.007$, and GLP1r $KD^{\Delta Nkx2.1}$, $P = 0.044$) in DIO wt and GLP1r $KD^{\Delta Nkx2.1}$ mice in a similar manner, as reflected by fasting glucose and OGTT assessment (Fig. 5*G* and *H*).

For further substantiation of the importance of central GLP1 signaling in the responses to AMP-DNM, DIO wt mice were fed with AMP-DNM (HFD+AMP-DNM) with icv administration of aCSF and another group was icv infused with exendin-9 (HFD+AMP-DNM+ex9), an antagonist of GLP1r (23). The minipump attached to the brain infusion cannula via a catheter assured continuous icv infusion of a dose of exendin-9 that is known to only block central (but not peripheral) GLP1r (24). Regarding food intake, exendin-9 per se caused no significant changes (HFD 2.69 ± 0.19 g and HFD+ex9 3.05 ± 0.24 g). However, DIO mice fed with AMP-DNM showed a decrease in food intake that was largely inhibited by icv exendin-9 (Fig. 6*A*). These findings further confirm the role of central GLP1r in the reduction of food intake induced by AMP-DNM. icv exendin-9 did not change the RER reductions by AMP-DNM (data not shown) and caused no changes in AMP-DNM–induced body weight reduction and loss of fat mass and gWAT weight (Fig. 6*B* and *C*). Similarly, icv exendin-9 did not affect the AMP-DNM–improved glucose tolerance in DIO wt mice (Fig. 6*D* and *E*).

Since AMP-DNM administration increased hypothalamic ARC and DMH neuronal activation in *ob/ob* mice, we comparatively assessed hypothalamic C-Fos activation in wt and GLP1r $KD^{\Delta Nkx2.1}$ DIO mice fed with AMP-DNM. DIO wt mice receiving AMP-DNM showed a higher C-Fos activation in the ARC and DMH (Fig. 5*I* and *J*). On the other hand, AMP-DNM did not affect C-Fos activation in the ARC or DMH of DIO GLP1r $KD^{\Delta Nkx2.1}$ mice on HFD (Fig. 5*I* and *J*). Consistently, POMC mRNA expression was higher in the hypothalamus and PPG expression in the brainstem was increased in DIO wt mice fed with AMP-DNM (Fig. 5*K* and *L*). These AMP-DNM–induced increases were not observed in the DIO GLP1r $KD^{\Delta Nkx2.1}$ mice (Fig. 5*K* and *L*), indicating that the brain GLP1r is necessary for

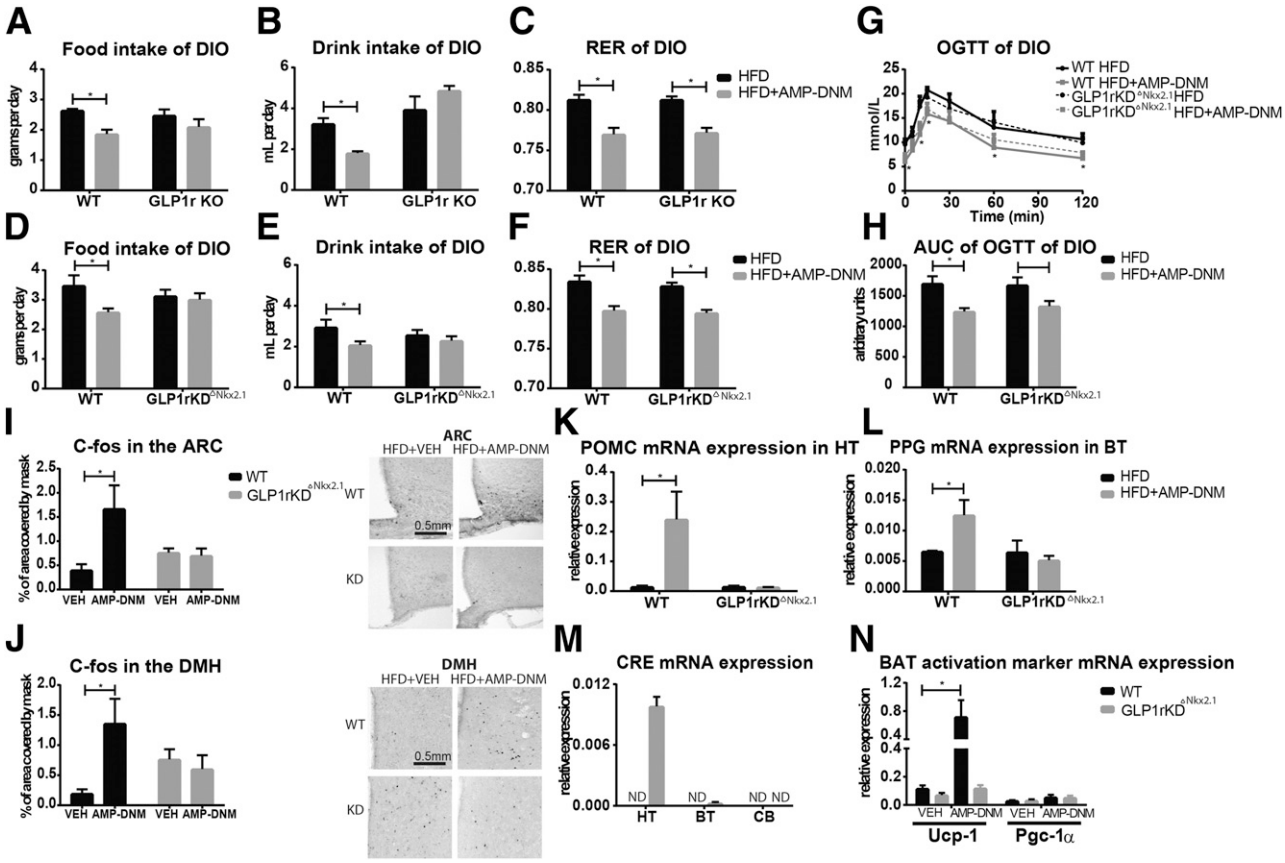

Figure 5— Brain GLP1r mediates the satiety effect and hypothalamic activation induced by AMP-DNM in obese mice. *A*: Daily food intake of wt and GLP1r KO DIO mice. *B*: Daily water intake of wt and GLP1r KO DIO mice. *C*: RER of wt and GLP1r KO DIO mice. *D*: Daily food intake of wt and GLP1r KD$^{\Delta Nkx2.1}$ DIO mice. *E*: Daily drink intake of wt and GLP1r KD$^{\Delta Nkx2.1}$ DIO mice. *F*: RER of wt and GLP1r KD$^{\Delta Nkx2.1}$ DIO mice. *G* and *H*: Plasma glucose levels and AUC after an OGTT in wt and GLP1r KD$^{\Delta Nkx2.1}$ DIO mice after 21-day diet. *I*: Percentage of ARC area covered by C-Fos mask and representative images of C-Fos staining in the ARC of wt and GLP1r KD$^{\Delta Nkx2.1}$ DIO (KD) mice after 21-day diet. *J*: Percentage of DMH area covered by C-Fos mask and representative images of C-Fos staining in the DMH of wt and GLP1r KD$^{\Delta Nkx2.1}$ mice after 21-day diet. *K*: POMC mRNA expression in the hypothalamus (HT) of wt and GLP1r KD$^{\Delta Nkx2.1}$ DIO mice. *L*: PPG mRNA expression in the brainstem (BT) of wt and GLP1r KD$^{\Delta Nkx2.1}$ DIO mice. *M*: Cre mRNA expression in the hypothalamus, brainstem, and cerebellum (CB) of wt and GLP1r KD$^{\Delta Nkx2.1}$ mice. ND, not detected. *N*: Ucp-1 and Pgc1-α mRNA expression in the BAT of wt and GLP1r KD$^{\Delta Nkx2.1}$ DIO mice. In brain images, the scale bar represents 0.5 mm. VEH, vehicle administration. *$P < 0.05$.

the stimulation of brainstem-hypothalamic anorexigenic neuropeptides by AMP-DNM.

AMP-DNM Stimulates BAT Activity Through Central GLP1 Signaling Pathway

The central GLP1 system has been implicated in the control of BAT activation and thermogenesis (9,25). We therefore tested the involvement of the central GLP1 system in BAT activation induced by AMP-DNM. We performed intravenous infusions of [^{14}C]DG and glycerol TRL-like emulsion particles in DIO HFD+AMP-DNM and DIO HFD+AMP-DNM+ex9 mice and monitored glucose and fatty acid uptake in different organs. DIO HFD+AMP-DNM mice showed increased [^{14}C]DG ($P = 0.01$) and [^{3}H]oleate uptake, specifically in iBAT. Both increases were not seen in DIO HFD+AMP-DNM+ex9 mice (Fig. 6*F* and *G*). Thus, the central GLP1r mediates the increase in glucose and TG uptake in the iBAT induced by AMP-DNM.

HFD+AMP-DNM iBAT also showed increased TH signal (Fig. 6*H*) and significantly increased thermogenic *Ucp-1* and *Pgc-1α* gene expression (Fig. 6*I* and *J*). DIO HFD+AMP-DNM+ex9 mice did not present this as clearly (Fig. 6*H–J*). These data suggest that icv exendin-9 administration blunted the increased sympathetic input and thermogenic gene expression in BAT after AMP-DNM exposure. Similarly, the BAT of DIO GLP1r KD$^{\Delta Nkx2.1}$ mice fed with AMP-DNM presented no increase in *Ucp-1* expression (Fig. 5*N*).

DISCUSSION

In the current study, we show that the gut-brain GLP1 pathway is a key mediator for AMP-DNM induced beneficial metabolic effects in obese mice. Oral administration of the iminosugar AMP-DNM results in a reduction of food intake, which is accompanied by an increase in plasma GLP1, in both mice and rats. We demonstrate that through stimulating GLP1 secretion from gut and acting on the CNS, the peripherally administrated AMP-DNM is

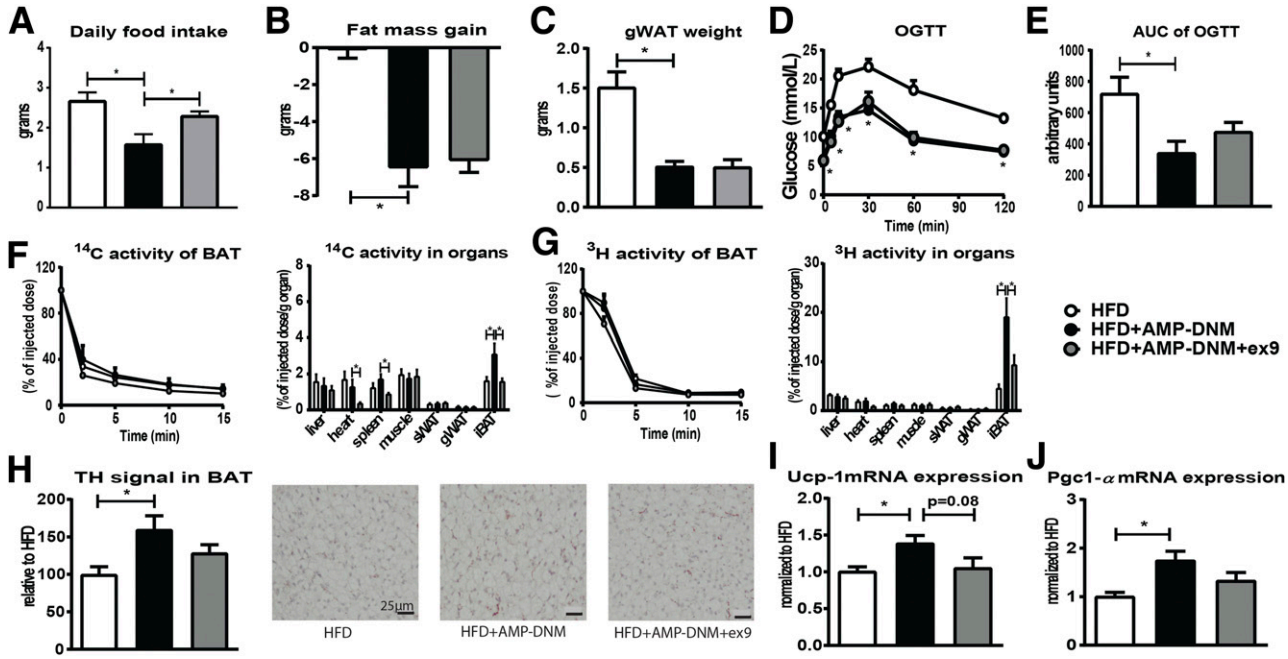

Figure 6—Brain GLP1r mediates the BAT activation induced by AMP-DNM in obese mice. *A*: Daily food intake. *B* and *C*: Difference in fat mass gain and gWAT pad weight. *D* and *E*: Plasma glucose levels and AUC of OGTT. *F*: Plasma ^{14}C activity decay and tissue ^{14}C activity uptake. *G*: Plasma ^{3}H activity decay and tissue ^{3}H activity uptake. *H*: TH signal quantification and representative images of TH staining of iBAT. Scale bar: 25 µm. *I*: *Ucp-1* mRNA expression in iBAT. *J*: *Pgc1-α* mRNA expression in iBAT. *$P < 0.05$.

essential to trigger changes in energy intake by significantly reducing food intake, correcting blood glucose levels, and increasing fat oxidation in obese rodents. Moreover, this AMP-DNM–gut–GLP1–CNS pathway also induces BAT activation, as demonstrated by increased glucose and TG-derived fatty acids uptake. We illustrate the essential role of the central GLP1 pathway by showing lack of reduction of food take and BAT activation after ingestion of an AMP-DNM–containing diet both in mice lacking the GLP1r in the forebrain and in mice chronically icv infused with an antagonist of the GLP1r.

We previously reported that AMP-DNM treatment improves insulin sensitivity, corrects glycemic control, and reduces food intake in *ob/ob* mice (4,5,26) and obese diabetic rats (4). In addition, orally administered AMP-DNM has been shown to lower brain GSLs and inhibit the cellular enzyme GBA2, indicating that AMP-DNM may enter the brain and inhibit its target enzymes (27). The improvement in insulin sensitivity is partly mediated by AMP-DNM inhibition of glycosidases processing food polysaccharides, buffering sugar assimilation (4) and reduced GSL synthesis, which counteracts insulin resistance stemming from excessive gangliosides (1). In particular, excessive GM3 is thought to interfere with insulin signaling (26). Here we show that in addition to its capacity as an enzyme inhibitor of GSL metabolism, AMP-DNM modulates energy metabolism through influencing endocrine factors acting on brain neural circuits controlling energy metabolism. Specifically, we demonstrate that ig administration of AMP-DNM increased the plasma level of active GLP1 in both lean and obese rodents. GLP1 is synthesized in the whole intestine by enteroendocrine L cells and in the NTS in the brainstem after nutrient ingestion (28) and subsequently modulates numerous physiological functions, improving glucose metabolism and stimulating satiety.

Importantly, GLP1 mimetics have been proven to be beneficial for body weight loss and treating type 2 diabetes (29). The specific neural circuit mediating the satiety effect induced by AMP-DNM still needs to be elucidated, but oral administration of AMP-DNM modulated POMC expression in the ARC and CRH expression in the PVN. In both these regions, GLP1r is expressed by neurons (30), and activation of these neurons is known to have anorexigenic effects (31–33). Besides the hypothalamic pathways, we also found increased C-Fos expression in the caudal part of the NTS and in the AP and a concomitant activation of PPG (precursor protein of GLP1) neurons in the NTS in the brainstem. It has previously been shown that peripheral administration of GLP1 or its agonist exendin-4 increases C-Fos expression in the caudal part of the NTS and in the AP (34). As one of the prominent circumventricular organs, activation of the AP has been implicated in the satiating effect of the blood-borne GLP1 (35–37). Thus, our data suggest that besides peripheral GLP1, the anorexigenic effect of AMP-DNM might also be mediated via the GLP1-producing neurons and their projections to different forebrain regions, including the PVN, DMH, and ARC (28). Indeed, optogenetic and

chemogenetic activation of GLP1 neurons in the NTS reduces food intake and body weight gain through simulation of the GLP1r-expressing CRH neurons in the PVN (33,38). Collectively, it is plausible that AMP-DNM stimulates both gut and brainstem GLP1 synthesis and that brainstem-derived GLP1 further acts on the hypothalamic circuits to mediate satiety as induced by AMP-DNM.

The NTS receives sensory vagal inputs and constitutes a major neuronal connection between the gut and the brain (39). Accumulating evidence has suggested that vagal afferents play an important role in mediating the anorectic effects of peripheral GLP1 (21). Sensory vagal afferents express GLP1 receptors, and peripheral GLP1 induces electrical activity in the vagus nerve (40). Gut-derived GLP1 might bind to GLP1 receptors present on vagal afferents in portal vein and activate neurons at the level of the dorsal motor nucleus of the vagus and NTS in the brainstem (41,42). Moreover, evidence collected from human studies has suggested that intravenous administration of GLP1 requires intact vagal nerve endings in order to reduce food intake (43). Therefore, AMP-DNM might exert its satiety effects by combinatorial gut-brain GLP1 pathways and vagus nerve activation may be an essential part of this communication.

Increased BAT activity is known to improve glucose metabolism and decrease body weight in obese mice (13,14). AMP-DNM markedly increased glucose and TG-derived fatty acid uptake specifically in the BAT and decreased lipid droplet content within brown adipocytes, similar to direct activation of brown adipocytes with a β3-adrenergic receptor agonist (15,44). A concomitantly increased TH signal, an indicator of sympathetic activity and expression of thermogenic *Ucp-1* and *Pgc-1α* in BAT, supports a functional activation of BAT of obese mice by AMP-DNM. We demonstrated that AMP-DNM activation of central GLP1r governed BAT activation. It was previously shown that the central GLP1 system has also been implicated in the control of BAT activation and thermogenesis control by increasing sympathetic output to the BAT (9,25). Accordingly, we showed that AMP-DNM increased C-Fos expression in the DMH neurons. As part of the neuroanatomical circuit modulating sympathetic innervation to BAT, activation of DMH neurons is important for GLP1-induced BAT thermogenesis (45) and that they might be important mediators for AMP-DNM induced BAT activation.

Several reports have suggested that both brain and peripheral GLP1 receptors are important mediators of GLP1 modulation of body glucose metabolism (10,21,24). Interestingly, the beneficial effects of AMP-DNM on glycemic control were not prevented by genetic ablation of central GLP1r or its blockade by exendin-9, suggesting possible peripheral GLP1r-mediated actions of AMP-DNM. Therefore, the decrease in food intake and BAT activation induced by AMP-DNM in obese mice, but not the corrections in glucose homeostasis, are critically dependent on central GLP1r. This is in line with the previous observation that brain GLP1r signaling only promotes satiety and does not lower blood glucose (7). A likely additional mechanism of action of GSL-lowering iminosugars is their documented positive effect on insulin sensitivity and insulin signaling (3). Of note, L-ido-AMP-DNM is less bitter than AMP-DNM and it triggers much poorer GLP1 release in the STC1 cells. L-ido-AMP-DNM treatment of obese rats only improves glucose metabolism—not other metabolic parameters. These findings further support the notion that the insulin-sensitizing effect of GSL lowering, independent of GLP1, contributes to improved glucose homeostasis (3). Intriguingly, similar improvements in glucose homeostasis in obese mice have been observed after GLP1 release stimulation by D-allulose sugar analogs (46). Since allulose has a sweet taste, it is likely that yet a different mechanism underlies its effects.

Induction of GLP1 secretion by dietary and gut microbiota–derived metabolites is generally attributed to the activation of fatty acid receptors, as well as the calcium-sensing receptor and the bile acid–sensing TGR5 receptor at the basolateral membrane (29). Interestingly, some bitter agents also potently induce secretion of GLP1 (16,17). In an earlier study, we were able to demonstrate the expression of the ortholog bitter receptor T2R118 in the intestine of mice (20). Jeon et al. (17) had previously shown the expression of T2R118 in mouse STC1 cells. After overexpression of endogenous bitter taste receptors in STC1 cells, we observed that AMP-DNM induces GLP1 secretion by interacting with mouse bitter taste receptor T2R118. Similar mechanisms have previously been shown by activation of bitter taste receptor T2R138, which results in the stimulation of GLP1 release from enteroendocrine L cells (29). Humans also release plasma GLP1 upon exposure to bitter compounds, and AMP-DNM does taste bitter. Our in vitro findings with modified STC1 cells do not prove that the same mechanism is relevant in vivo in mice orally treated with AMP-DNM. However, our current findings warrant further investigations into this possibility. Of note, our study with AMP-DNM was conducted with rodents. Extrapolating findings made with these animals to possible similar responses in humans should be done with great caution. It is warranted to study the expression of bitter receptors like hT2R16 in the intestinal L cells.

In conclusion, our investigation shows that AMP-DNM exerts concerted and pleiotropic beneficial action onto energy intake, BAT activation, and glucose homeostasis through both GLP1-dependent and -independent pathways. Our findings provide a mechanistic basis by which AMP-DNM could serve as combinatorial yet complementary pharmacological strategy together with GLP1 agonists to treat metabolic diseases with obesity and type 2 diabetes at the core.

Acknowledgments. The authors thank Joop van Heerikhuize (Netherlands Institute for Neuroscience, Amsterdam, the Netherlands) for technical support with the laser capture microscopy and imaging.

Funding. This work was supported by the European Research Council Advanced Grant CHEMSPHINGO to H.O. and J.M.F.G.A., by a Dutch Heart

Foundation Established Investigator grant (2009T038) to P.C.N.R., and by the Netherlands Cardiovascular Research Initiative (CVON2017-20), an initiative with support of the Dutch Heart Foundation for the GENIUS-II project to P.C.N.R. Y.W. is supported by a ZonMW-VENI grant (91617027). C.-X.Y. is supported by an Academic Medical Center fellowship (2014) and the Dutch Diabetes Research Foundation (2015.82.1826).

Duality of Interest. R.J.S. provides research support at Ethicon Endo-Surgery/Johnson & Johnson, Janssen/Johnson & Johnson, MedImmune, Boehringer Ingelheim, and Sanofi and acts as consultant/Scientific Advisory Board at Ethicon Endo-Surgery/Johnson & Johnson, Orexigen, Novo Nordisk, Daiichi Sankyo, Janssen/Johnson & Johnson, Novartis, Paul Hastings Law Firm, Zafgen, Takeda, and Boehringer Ingelheim. No other potential conflicts of interest relevant to this article were reported.

Author Contributions. D.H.M.C. and Y.W. contributed to designing research, performing experiments, analyzing data, interpreting results of experiments, preparing figures, and drafting the manuscript. E.F., R.O., C.v.R., E.T.P., M.v.E., M.V., R.B., A.R.M., S.S., M.M., S.K., K.J., D.W., and C.M. contributed to performing experiments. R.J.S. and M.H.T. contributed to editing and revising the manuscript. H.O. contributed to providing iminosugars and editing and revising the manuscript. P.C.N.R. contributed to conception of part of the research, interpreting results of experiments, and editing and revising the manuscript. A.K. contributed to conception of part of the research and to editing and revising manuscript. J.M.F.G.A. contributed to conception of the research project, drafting the manuscript, and approving the final version of the manuscript. C.-X.Y. contributed to conception of part of the research, editing and revising the manuscript, and approving the final version of manuscript. J.M.F.G.A. is the guarantor of this work and, as such, had full access to all the data in the study and takes responsibility for the integrity of the data and the accuracy of the data analysis.

References

1. Aerts JM, Boot RG, van Eijk M, et al. Glycosphingolipids and insulin resistance. Adv Exp Med Biol 2011;721:99–119
2. Wennekes T, van den Berg RJ, Boot RG, van der Marel GA, Overkleeft HS, Aerts JM. Glycosphingolipids–nature, function, and pharmacological modulation. Angew Chem Int Ed Engl 2009;48:8848–8869
3. Aerts JM, Ottenhoff R, Powlson AS, et al. Pharmacological inhibition of glucosylceramide synthase enhances insulin sensitivity. Diabetes 2007;56:1341–1349
4. Wennekes T, Meijer AJ, Groen AK, et al. Dual-action lipophilic iminosugar improves glycemic control in obese rodents by reduction of visceral glycosphingolipids and buffering of carbohydrate assimilation. J Med Chem 2010;53:689–698
5. van Eijk M, Aten J, Bijl N, et al. Reducing glycosphingolipid content in adipose tissue of obese mice restores insulin sensitivity, adipogenesis and reduces inflammation. PLoS One 2009;4:e4723
6. Bijl N, Sokolović M, Vrins C, et al. Modulation of glycosphingolipid metabolism significantly improves hepatic insulin sensitivity and reverses hepatic steatosis in mice. Hepatology 2009;50:1431–1441
7. Sisley S, Gutierrez-Aguilar R, Scott M, D'Alessio DA, Sandoval DA, Seeley RJ. Neuronal GLP1R mediates liraglutide's anorectic but not glucose-lowering effect. J Clin Invest 2014;124:2456–2463
8. Girault EM, Alkemade A, Foppen E, Ackermans MT, Fliers E, Kalsbeek A. Acute peripheral but not central administration of olanzapine induces hyperglycemia associated with hepatic and extra-hepatic insulin resistance. PLoS One 2012;7:e43244
9. Kooijman S, Wang Y, Parlevliet ET, et al. Central GLP-1 receptor signalling accelerates plasma clearance of triacylglycerol and glucose by activating brown adipose tissue in mice. Diabetologia 2015;58:2637–2646
10. Knauf C, Cani PD, Perrin C, et al. Brain glucagon-like peptide-1 increases insulin secretion and muscle insulin resistance to favor hepatic glycogen storage. J Clin Invest 2005;115:3554–3563
11. Frayn KN. Calculation of substrate oxidation rates in vivo from gaseous exchange. J Appl Physiol 1983;55:628–634
12. Scrocchi LA, Brown TJ, MaClusky N, et al. Glucose intolerance but normal satiety in mice with a null mutation in the glucagon-like peptide 1 receptor gene. Nat Med 1996;2:1254–1258
13. Stanford KI, Middelbeek RJ, Townsend KL, et al. Brown adipose tissue regulates glucose homeostasis and insulin sensitivity. J Clin Invest 2013;123:215–223
14. Bartelt A, Heeren J. Adipose tissue browning and metabolic health. Nat Rev Endocrinol 2014;10:24–36
15. Hoeke G, Kooijman S, Boon MR, Rensen PC, Berbée JF. Role of brown fat in lipoprotein metabolism and atherosclerosis. Circ Res 2016;118:173–182
16. Jang HJ, Kokrashvili Z, Theodorakis MJ, et al. Gut-expressed gustducin and taste receptors regulate secretion of glucagon-like peptide-1. Proc Natl Acad Sci USA 2007;104:15069–15074
17. Jeon TI, Zhu B, Larson JL, Osborne TF. SREBP-2 regulates gut peptide secretion through intestinal bitter taste receptor signaling in mice. J Clin Invest 2008;118:3693–3700
18. Bufe B, Hofmann T, Krautwurst D, Raguse JD, Meyerhof W. The human TAS2R16 receptor mediates bitter taste in response to beta-glucopyranosides. Nat Genet 2002;32:397–401
19. Sakurai T, Misaka T, Ueno Y, et al. The human bitter taste receptor, hTAS2R16, discriminates slight differences in the configuration of disaccharides. Biochem Biophys Res Commun 2010;402:595–601
20. Herrera Moro Chao D, Argmann C, Van Eijk M, et al. Impact of obesity on taste receptor expression in extra-oral tissues: emphasis on hypothalamus and brainstem. Sci Rep 2016;6:29094
21. Barrera JG, Sandoval DA, D'Alessio DA, Seeley RJ. GLP-1 and energy balance: an integrated model of short-term and long-term control. Nat Rev Endocrinol 2011;7:507–516
22. Pan Q, Li C, Xiao J, et al. In vivo characterization of the Nkx2.1 promoter/enhancer elements in transgenic mice. Gene 2004;331:73–82
23. Göke R, Fehmann HC, Linn T, et al. Exendin-4 is a high potency agonist and truncated exendin-(9-39)-amide an antagonist at the glucagon-like peptide 1-(7-36)-amide receptor of insulin-secreting beta-cells. J Biol Chem 1993;268:19650–19655
24. Parlevliet ET, de Leeuw van Weenen JE, Romijn JA, Pijl H. GLP-1 treatment reduces endogenous insulin resistance via activation of central GLP-1 receptors in mice fed a high-fat diet. Am J Physiol Endocrinol Metab 2010;299:E318–E324
25. Lockie SH, Heppner KM, Chaudhary N, et al. Direct control of brown adipose tissue thermogenesis by central nervous system glucagon-like peptide-1 receptor signaling. Diabetes 2012;61:2753–2762
26. Inokuchi JI, Inamori KI, Kabayama K, et al. Biology of GM3 ganglioside. Prog Mol Biol Transl Sci 2018;156:151–195
27. Marques AR, Aten J, Ottenhoff R, et al. Reducing GBA2 activity ameliorates neuropathology in Niemann-Pick type C mice. PLoS One 2015;10:e0135889
28. Baggio LL, Drucker DJ. Glucagon-like peptide-1 receptors in the brain: controlling food intake and body weight. J Clin Invest 2014;124:4223–4226
29. Engelstoft MS, Schwartz TW. Opposite regulation of ghrelin and glucagon-like peptide-1 by metabolite G-protein-coupled receptors. Trends Endocrinol Metab 2016;27:665–675
30. Cork SC, Richards JE, Holt MK, Gribble FM, Reimann F, Trapp S. Distribution and characterisation of glucagon-like peptide-1 receptor expressing cells in the mouse brain. Mol Metab 2015;4:718–731
31. Sandoval DA, Bagnol D, Woods SC, D'Alessio DA, Seeley RJ. Arcuate glucagon-like peptide 1 receptors regulate glucose homeostasis but not food intake. Diabetes 2008;57:2046–2054
32. Secher A, Jelsing J, Baquero AF, et al. The arcuate nucleus mediates GLP-1 receptor agonist liraglutide-dependent weight loss. J Clin Invest 2014;124:4473–4488

33. Liu J, Conde K, Zhang P, et al. Enhanced AMPA receptor trafficking mediates the anorexigenic effect of endogenous glucagon-like peptide-1 in the paraventricular hypothalamus. Neuron 2017;96:897–909.e5
34. Baraboi ED, St-Pierre DH, Shooner J, Timofeeva E, Richard D. Brain activation following peripheral administration of the GLP-1 receptor agonist exendin-4. Am J Physiol Regul Integr Comp Physiol 2011;301:R1011–R1024
35. Baumgartner I, Pacheco-López G, Rüttimann EB, et al. Hepatic-portal vein infusions of glucagon-like peptide-1 reduce meal size and increase c-Fos expression in the nucleus tractus solitarii, area postrema and central nucleus of the amygdala in rats. J Neuroendocrinol 2010;22:557–563
36. Kawatani M, Yamada Y, Kawatani M. Glucagon-like peptide-1 (GLP-1) action in the mouse area postrema neurons. Peptides 2018;107:68–74
37. Punjabi M, Arnold M, Rüttimann E, et al. Circulating glucagon-like peptide-1 (GLP-1) inhibits eating in male rats by acting in the hindbrain and without inducing avoidance. Endocrinology 2014;155:1690–1699
38. Gaykema RP, Newmyer BA, Ottolini M, et al. Activation of murine preproglucagon-producing neurons reduces food intake and body weight. J Clin Invest 2017;127:1031–1045
39. Grill HJ, Hayes MR. Hindbrain neurons as an essential hub in the neuroanatomically distributed control of energy balance. Cell Metab 2012;16:296–309
40. Bucinskaite V, Tolessa T, Pedersen J, et al. Receptor-mediated activation of gastric vagal afferents by glucagon-like peptide-1 in the rat. Neurogastroenterol Motil 2009;21:978-e78
41. Trapp S, Richards JE. The gut hormone glucagon-like peptide-1 produced in brain: is this physiologically relevant? Curr Opin Pharmacol 2013; 13:964–969
42. Hisadome K, Reimann F, Gribble FM, Trapp S. Leptin directly depolarizes preproglucagon neurons in the nucleus tractus solitarius: electrical properties of glucagon-like peptide 1 neurons. Diabetes 2010;59: 1890–1898
43. Plamboeck A, Veedfald S, Deacon CF, et al. The effect of exogenous GLP-1 on food intake is lost in male truncally vagotomized subjects with pyloroplasty. Am J Physiol Gastrointest Liver Physiol 2013;304:G1117–G1127
44. Berbée JF, Boon MR, Khedoe PP, et al. Brown fat activation reduces hypercholesterolaemia and protects from atherosclerosis development. Nat Commun 2015;6:6356
45. Lee AA, Owyang C. Sugars, sweet taste receptors, and brain responses. Nutrients 2017;9:1–13
46. Iwasaki Y, Sendo M, Dezaki K, et al. GLP-1 release and vagal afferent activation mediate the beneficial metabolic and chronotherapeutic effects of D-allulose. Nat Commun 2018;9:113